A Two-Dimensional Coupled Biosphere-Atmosphere Model and Its Application

Yongkang Xue

Center for Oceans-Land-Atmosphere Interactions Department of Meteorology, University of Maryland, College Park, MD 20742 U. S. A.

Received January 22, 1991; revised March 29, 1991

ABSTRACT

A 2-D zonally averaged, time dependent climate model is developed to study the biosphere-atmosphere interaction. A numerical scheme is specifically designed for the model to ensure the conservation of mass, momentum, energy, and water vapor. A simple parameterization of vegetation-soil layers is incorporated in this 2-D model. Using this coupled model, we study the biosphere and atmosphere interaction. Some preliminary results concerning the African drought with annual mean conditions are presented.

I. INTRODUCTION

After more than a decade sustained work in global climate change studies, more scientists have reached a concession that the variation of land surface characteristics can have a significant impact on the climate. To have a better understanding of this effect, more elaborate and biologically realistic surface models have been deveploped by Dickinson (1984) and Sellers et al. (1986). While they shared the similar philosophy, these two models are different in detail. The first one, called Biosphere-Atmosphere Transfer Scheme (BATS), was coupled to the NCAR Community Climate Model (Dickinson et al. 1986). The later one, called Simple Biosphere Model (SiB), was implemented in a GCM by Sato et al. (1989), and simplified by Xue et al. (1991). Using these models, some experiments have been carried out to investigate Amazon deforestation (Dickinson and Henderson-Sellers, 1988, Shukla et al., 1990), and African desertification (Xue et al., 1990).

Most experiments of land-atmosphere interaction were carried out in GCMs. It is more realistic. However, a GCM usually takes more than a decade to develop and it needs a huge amount of computer time. Meanwhile, a two-dimensional model has the advantage of computational economy and, at the same time, many physical processes may be explicitly included in the model.

A two-dimensional zonal climate model has been developed in this study and briefly described in Section 2. This model conserves atmospheric energy, momentum, air mass, and water vapor. In connection with the 2-D climate model, we have incorporated two soil layers and one vegetation layer to evaluate the transphort of sensible and latent heat flux from the surface. Based on the scheme proposed by Dickinson (1984), and Dickinson et al. (1986) with various degrees of simplicity, a vegetation model in snow-free land surface has been presented in Section 3. A numerical scheme was specifically designed for the model to ensure the conservation of energy and water vapor. It is presented in Section 4. The application of this model in African drought study is briefly introduced in Section 5.

II. THE 2-D MODEL

We developed a 19-layer, zonally averaged 2-D climate model for the biosphere-atmosphere interaction study. A spherical coordinate system is used horizontally and a pressure system vertically. The mean field governing equations are the momentum equations, thermodynamic equation, water vapor equation, continuity equation, and hydrostatic equation (Xue et al. 1990).

The vertical eddy flux and horizontal diffusion play important roles in the 2-D model. The vertical eddy flux for momentum, temperature, and specific humidity may be parameterized in the forms

$$\tau_x = -\rho K \frac{\partial X}{\partial z} \ , \tag{2.1}$$

where X can be u or v, which are the wind velocity components in longitude and latitude, respectively, or q, the specific humidity, and

$$\tau_T = -\rho K_T \left[\frac{1000}{p}\right]^{\frac{R}{C_p}} \left[\frac{\partial \theta}{\partial z} - \gamma_c\right] \ , \tag{2.2}$$

where ρ the air density, R the gas constant for air, γ_c the countergradient lapse rate (Deardorff, 1972), θ the potential temperature. Following Oliger et al. (1970), we set eddy viscosity, eddy thermal diffusion coefficient, and eddy water vapor diffusion coefficient equal in the model, and take

$$K = \begin{cases} 20 + 100\left\{1 - \exp\left[600\left(\dfrac{\partial \theta}{\partial z} - \gamma_c\right)\right]\right\}, & \dfrac{\partial \theta}{\partial z} < \gamma_c \\ \dfrac{20}{1 + 40R_i} + A, & \dfrac{\partial \theta}{\partial z} > \gamma_c \end{cases} \tag{2.3}$$

where the unit for K is $m^2\ s^{-1}$ and R_i is the bulk Richardson number given by

$$R_i = \frac{g}{T}\left(\frac{\partial \theta}{\partial z} - \gamma_c\right) \Big/ \left[\left(\frac{\partial u}{\partial z}\right)^2 + \left(\frac{\partial v}{\partial z}\right)^2 + 10^{-12}\right] \ . \tag{2.4}$$

The countergradient lapse rate γ_c and A are taken to be 0.005 K/m and 2, respectively, for $p > 700$ hPa, while 0.001 K/m and 0.1 are assumed otherwise.

The parameterization of the horizontal diffusion has been extensively studied in the past. Following Holloway and Manabe (1970) and Oliger et al. (1970), the diffusion terms for momentum in the spherical coordinate may be written in the forms

$$F_u = \frac{1}{\mu}\frac{\partial}{\partial y}\left[\mu^2 K_h \frac{\partial}{\partial y}(u - \bar{\omega}\mu)\mu\right] \ , \tag{2.5}$$

$$F_v = \frac{\partial}{\partial y}\left[\mu K_h \frac{\partial (v\mu)}{\partial y}\right] - \frac{\tan\varphi}{a} K_h \left[\frac{\partial (v\mu)}{\partial y}\right] \ , \tag{2.6}$$

where $y = a\sin\varphi$, a the radius of the earth, φ the latitude, $\mu = \cos\varphi$, K_h is the horizontal diffusivity, which is assumed to be the same for momentum, heat, and water vapor fluxes. It is parameterized in the form

$$K_h = C_h (a\Delta\varphi)^2 \sqrt{[\partial(v\mu)/\partial y]^2 + [\partial(u\mu)/\partial y]^2} \ . \tag{2.7}$$

The coefficient C_h is to be determined empirically. The mean angular velocity is

$$\overline{\omega} = \int_{\varphi_s}^{\varphi_n} \frac{u}{\cos\varphi} d\varphi \ . \tag{2.8}$$

Where φ_n and φ_s are values of the latitude at the north and south boundaries, respectively.

The horizontal diffusion terms for temperature and specific humidity may be expressed by

$$F_x = \frac{\partial}{\partial y}[\mu^2 K_h \frac{\partial X}{\partial y}] \ , \tag{2.9}$$

where X may be T or q.

To prevent the superadiabatic lapse rates in the model, the convective adjustment was introduced in this model. For the saturated layer, the excess water vapor is rained out as precipitation and, at the same time, latent heat is added to the layer. The total precipitation is then the sum of all individual layer precipitation. The radiation package developed by Liou and Ou (1981, 1983) is used in the present model. The clouds are created in the model according to the relative humidity, which are used for radiation calculation (Xue et al. 1990).

III. MODELING OF BIOSPHERE MODEL

The biosphere model in this study is basically from those proposed by Deardorff (1978) and Dickinson (1984). A number of modifications were made. The snow cover is not considered in this study.

A single layer of vegetation which has negligible heat capacity and two soil layers are presented in this model. There are five prediction equations. The prognostic variables are total soil water content S_{tw}, surface water content S_{sw}, the ground temperature T_g, the subsurface temperature T_d, and the water stored on foliage W_f (Fig.1). The equations for water contents are based on the water balance on the ground and foliage. The force restoration method is used for the calculation of the ground temperature (Xue et al. 1990).

The vegetation–soil layer affects the radiative transfer at surface, the surface energy partition into sensible heat and latent heat flux, and momentum flux. The surface albedos are prescribed according to the observation data in our study. The calculation of the fluxes are based upon the energy balance.

The sensible and latent heat transport from the covered surface have very significant impact on the atmosphere. The vertical flux of water vapor from the canopy τ_{qs} and the heat flux from the vegetation layer $C_p\tau_{Ts}$ may be expressed by

$$\tau_{qs} = \rho_a C_D |\overline{V}|_a (q_{af} - q_a) \ , \tag{3.1}$$

$$C_p\tau_{Ts} = C_p \rho_a C_D |\overline{V}|_a (T_{af} - T_a) \ , \tag{3.2}$$

where ρ_a the air density, T_a and q_a are the air temperature and specific humidity at the surface, respectively, C_D the drag coefficient, $|V|_a$ the velocity. To obtain τ_{qs} and τ_{Ts} from Eqs. (3.1) and (3.2), T_a, q_a, and the temperature T_{af} and water vapor specified humidity q_{af} for air within the canopy must be known.

It is assumed that the heat capacity of air within the canopy is negligible. Thus, the heat flux from the foliage and ground must be balanced by the heat flux to the atmosphere. T_{af} can be calculated through this relationship. Also, we assume that the canopy air does not store water vapor. Hence, q_{af} can be calculated in a similar manner. The heat flux and water

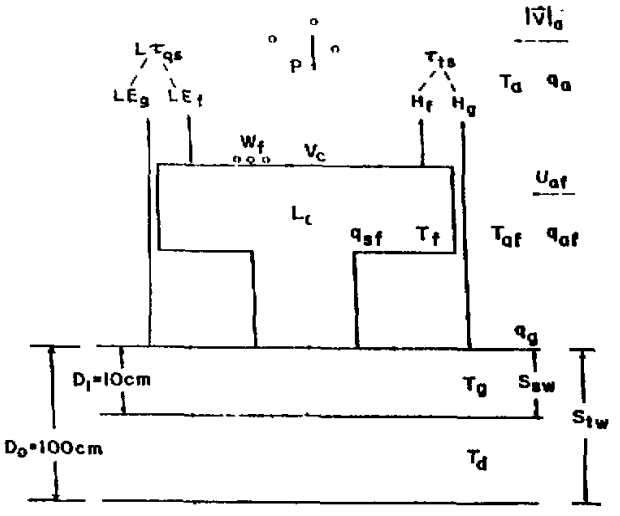

Fig.1. A schematic diagram denoting the components of the surface hydrological cycle. V_c is the vegetation cover, P the precipitation, T_a, T_{af}, T_f, T_g, and T_d the temperatures above the vegetation layer, within the foliage layer, of the foliage, at the surface soil, and subsurface, respectively, q_a and q_{af} the mixing ratios above and within the vegetation layer, respectively, q_{sf} and q_g the saturated mixing ratios at temperatures T_f and T_g, respectively, S_{sw} the surface soil water in the upper layer of soil, S_{tw} the total water in the rooting zone of soil, E_g and E_f fluxes of water vapor from the ground and foliage, respectively, H_g and H_f the sensible heat fluxes from the ground and foliage, respectively, L_c the leaf area index.

balance equations are

$$C_p \tau_{Ts} = H_f + H_g \ , \tag{3.3}$$

and

$$\tau_{qs} = E_f + E_g \ , \tag{3.4}$$

where the sensible heat fluxes from the foliage H_f and the ground H_g are given by

$$H_f = V_c C_f \sqrt{U_{af}}\, C_p (T_f - T_{af}) L_c \ , \tag{3.5}$$

where L_c is the sum of the leaf area index and the stem area index, and V_c the vegetation cover. These parameters are specified according to the vegetation types described in Dickinson et al. (1986).

$$H_g = \rho_a C_p C_D U_{af} (T_g - T_{af}) \ . \tag{3.6}$$

In Eq.(3.5), the foliage temperature T_f is introduced. This is a very important variable in the model for the calculation of energy exchanges involving infrared, sensible, and latent heat fluxes between the ground, the vegetation layer, and the atmosphere. It may be computed from the energy conservation equation for foliage (see Fig.1), as follows:

$$V_c[(1-\alpha)F_s^{\downarrow} + F_{IR}^{\downarrow} - \sigma T_g^4] - 2V_c\sigma(T_f^4 - T_g^4) = LE_f + H_f \ . \tag{3.7}$$

where α is the surface albedo, $F_s^{\downarrow}$ the downward solar surface flux, $F_{IR}^{\downarrow}$ the downward infrared flux. To solve for T_f, successive iterations must be performed. We found that in our experiments one iteration at each time step is sufficient to obtain a stable solution. The simple iterative procedure to obtain the solution for T_f appears to be appropriate in view of the fact that the surface–atmosphere system does not change dramatically within a time step of minutes. In the calculations, we have performed careful checks on this iterative procedure to ensure that the surface energy budget is conserved.

The water vapor flux from the ground, E_g, is the minimum of two quantities: the potential evaporation rate and maximum evaporation rate. The maximum evaporation rate is obtained from the parameterization proposed by Dickinson (1984). They were obtained by means of the dimensional analysis, physical reasoning, and trial–and–error numerical integrations. The equations have very complex forms. The potential evaporation rate is given by

$$E_q^{pot} = \rho_a C_D |\vec{V}|_a (q_g - q_{af}) \ , \tag{3.8}$$

where q_g the saturated specific humidity at the surface. The evaporation from the foliage is given by

$$E_f = \gamma'' E_f^w \ , \tag{3.9}$$

where γ'' represents the fraction of potential evaporation from a leaf and E_f^w is the evaporation of water from the wet foliage. γ'' is functions of the surface wetness, stomatal and root resistance, and surface air conditions (Dickinson, 1984). E_f^w may be expressed by

$$E_f^w = V_c L_c \rho_a C_f \sqrt{U_{af}} (q_f^s - q_{af}) \ , \tag{3.10}$$

where q_f^s is the saturation mixing ratio at the foliage temperature T_f.

We use the parameterization for the wind velocity U_{af} within the foliage layer, given by Dickinson et al. (1981), in the form

$$U_{af} = |\vec{V}|_a [(1.2\sqrt{C_d} - 1)V_c + 1] \ . \tag{3.11}$$

The coefficient of transfer between foliage and air in the foliage is taken to be (Deardorff, 1978)

$$C_f = 0.01(1 + 0.3 / U_{af}) \ . \tag{3.12}$$

This equation includes the effects of both forced and free convection. By assuming that the surface layer is in equilibrium, u_a, v_a be obtained from

$$K \left.\frac{\partial u}{\partial z}\right|_a = C_D u_a |\vec{V}|_a \ , \tag{3.13}$$

$$K \left.\frac{\partial v}{\partial z}\right|_a = C_D v_a |\vec{V}|_a \ . \tag{3.14}$$

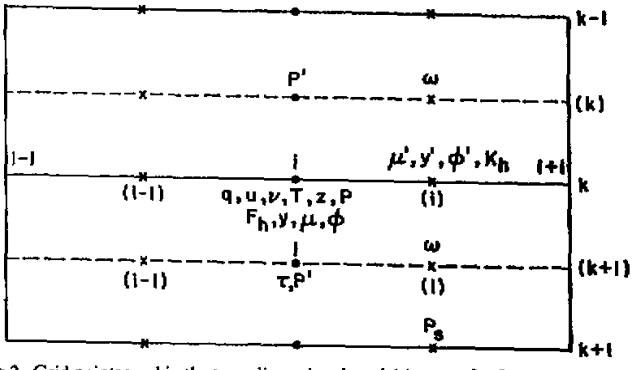

Fig.2. Grid points used in the two-dimensional model (see text for further explanation).

As for T_a and q_a, we must consider different ground conditions. For bare soil, the equilibrium equations may be expressed by

$$\left.\begin{aligned} K\left(\frac{\partial\theta}{\partial z}-\gamma_c\right) &= C_D(T_a-T_g)|\overline{V}|_a \\ K\frac{\partial q}{\partial z} &= C_D(q_a-q_g)|\overline{V}|_a \end{aligned}\right\}. \tag{3.15}$$

For the vegetation covered area, we have

$$\left.\begin{aligned} K\left(\frac{\partial\theta}{\partial z}-\gamma_c\right) &= C_D(T_a-T_{af})|\overline{V}|_a \\ K\frac{\partial q}{\partial z} &= C_D(q_a-q_{af})|\overline{V}|_a \end{aligned}\right\}. \tag{3.16}$$

IV. NUMERICAL SCHEME

The staggered grids are used in the numerical scheme, on which temperature, water vapor mixing ratio, and horizontal velocities are calculated. The vertical velocity are calculated at midpoints. A vertical pressure coordinate system is used, in which the atmosphere is divided into 19 layers extending to 100 hPa. Except for the lowest layer, the pressure between each level is 50 hPa. The temperature, water vapor, and horizontal velocity are calculated at 100 hPa, 150 hPa, etc. and the vertical velocity is calculated at midlevels (Fig.2). The time step used is 15 minutes.

The space differencing for the governing equations employed in the present model is a second-order explicit finite-difference scheme. This numerical method is based on the energy conserving difference scheme described by Haltiner and Williams (1980). However, improvements has been made to ensure the conservation. We first define the operator $L(F)$ in the form

$$L(F)=\frac{\partial(\mu VF)}{\partial y}+\frac{\partial(\omega F)}{\partial P}\ , \tag{4.1}$$

where F may be u, v, q, or T, and $\mu=\cos\varphi$. Let $v'=\mu v$, then the finite-difference approximation for $L(F)$ may be expressed by

$$L(F)|_{i,k}=\frac{1}{4[y'(i)-y'(i-1)]}\{[v'(i+1,k)+v'(i,k)][F(i+1,k)+F(i,k)]$$

$$-[v'(i,k)+v'(i-1,k)][F(i,k)+F(i-1,k)]\}$$
$$+\frac{1}{4(P'_{k+1}-P'_{k})}\{[\omega(i,k+1)+\omega(i-1,k+1)][F(i,k+1)+F(i,k)]$$
$$-[\omega(i,k)+\omega(i-1,k)][F(i,k)+F(i,k-1)]\}\ , \tag{4.2}$$

where P'_k is the pressure at 125 hPa, 175 hPa,etc., and $y'(i)$ is at the midpoint between $y(i)$ and $y(i+1)$. The variables u,v and ω are staggered not only in the vertical, but in the horizontal as well, as shown in Fig.2. This will guarantee that the sum of the terms $\partial(u\mu)/\partial y + \partial\omega/\partial p$, over the integration domain in the continuity equation, is equal to zero. The present scheme conserves the square of F (Xue, 1989).

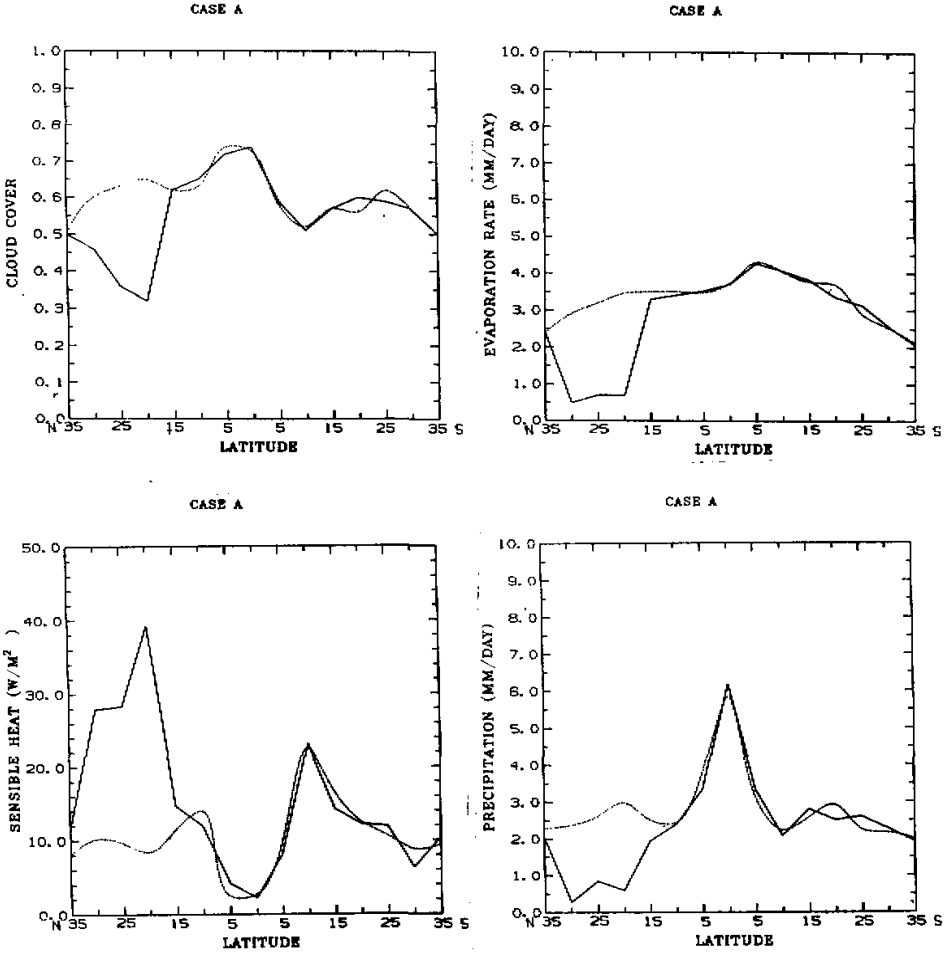

Fig.3. Comparison between results computed from the control run (solid line) and Case A (dash line). (a) Cloud cover, (b) evaporation rate (mm / d) , (c) sensible heat (W / M^2), (d) precipitation (mm / d).

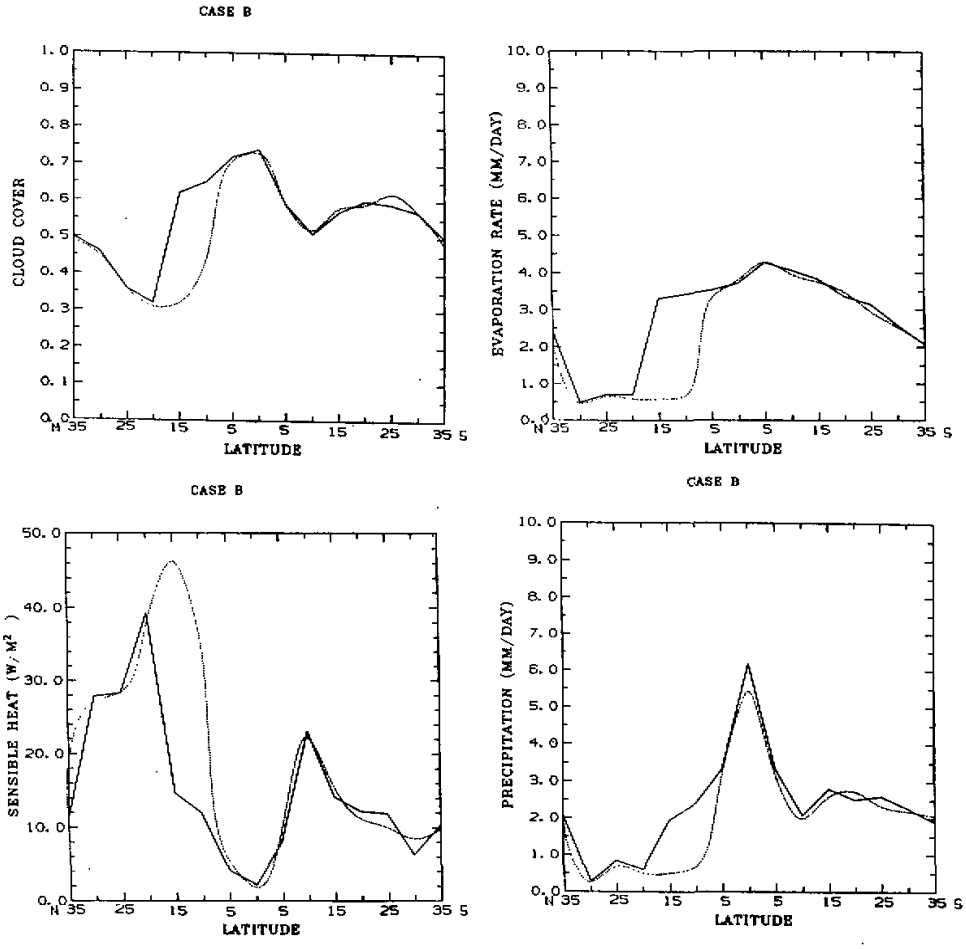

Fig.4. Comparison between results computed from the control run (solid line) and Case B (dash line). (a) Cloud cover, (b) evaporation rate (mm / d), (c) sensible heat (W / M^2), (d) precipitation (mm / d).

V. EXPERIMENTS

Since African climate has a significant zonal pattern, we used this model in the African drought studies (Xue et al., 1990). The 2–D model extends from 45°N to 45°S. The validation of this model has been discussed in that study in very detail. The results showed that the present 2–D model can, in general, simulate the African zonal climate pattern.

While this paper mainly focuses on the model presentation, we will briefly introduce some further results from African drought experiments. In the tropics the majority of the solar energy is absorbed by the earth and transferred to the atmosphere. The latent heat release and radiative heating are the main energy source. The surface perturbation should have much strong impact on atmosphere in tropics than in mid–latitude. Charney (1975) in his pioneer study used a 2–D model to study the albedo effects in Africa in summer and winter cases. He obtained similar response in both cases, but weaker feedback in winter. In our previous stud-

ies (Xue et al., 1990) we introduce the results with the diurnal variation in summer season. In this study, however, we will focus our discussion to the cases without diurnal variation in the annual mean condition.

There are oceans at the south of 35°S and north of 35°N in this model. We set the desert between 20°N and 30°N according to Matthews data (1985). Dickinson et al. (1986) introduced different vegetation parameter values for different vegetation types. Based upon these two data set we did the zonal average in different latitudes over African continent. The annually mean ocean temperatures are from the GFDL Atmospheric Circulation Tape Library, 1958–1973 (Oort, 1983), which are not interacted with the model. The albedo values are also taken from Matthews(1985). The zonal averaged albedos over the African are used in this study. The cosine of solar zenith angles in this experiment are annually averaged values.

The initial values in the experiments are from the GFDL tape library (Oort, 1983). These data, including temperature, humidity, and wind fields, as given for every 2.5° latitude and 5° longitude, are based on a ten–year mean (1963–1973). The global zonally averaged data for annual mean are used as the initial values for this experiment. Using this initial and boundary condition, the time integrations of the model were carried out for 45 days. The results for the last 30 days were averaged. This is called control run.

Using the present model, two sensitivity experiments were performed to study the response of atmosphere to surface conditions. In one experiment the whole desert in this model is replaced by vegetation. The albedo, roughness, and vegetation cover used are changed from about 0.24, 0.36 m, and 0.26 to 0.17, 0.75 m, and 0.8, respectively. The initial soil moisture is set to be 2 cm on the surface and 25 cm in the total soil layer in vegetated area instead of previous 1 cm and 10 cm. This experiment is called Case A. In another experiment the desert was extended to 10°N since desertification in African occurred primarily in the Sahel area. This extension, of coures, is designed to exaggerate the actual desertification in order to have computational significance. In that area those vegetation related parameters, i.e., leaf index et al., are set to zero. The soil type is changed from loam–like to sandy. The surface albedo of extended desert is changed from about 0.17 to 0.3. The roughness length is 0.01M instead of 0.75M. This experiment is called Case B. These results will be used to compare the results from control run.

After desert expended or desert removed, sensible heat, latent heat, cloud cover, and precipitation changed significantly. The comparisons of these quantities in Case A were shown in Fig.3. The comparisons for Case B were in Fig. 4. When desert was removed, the averaged cloud cover in tested area increased 0.25. The sensible heat decreased 23 W/M^2. The latent heat increased 74 W/M^2 (i.e., 2.6 mm / day). The precipitation increased 2.1 mm / day. While the desert was expended, the averaged cloud cover in the tested area decreased 0.26. The sensible heat increased 28 W/M^2. The latent heat decreased 80 W/M^2, i.e., 2.7 mm / day. The precipitation decreased 1.6 mm / day. Clearly, the decrease of the vertical moisture transfer plays a crucial role in the reduction of rainfall in these two experiments. In Charney et al'.s GCM experiment (1977) after albedo increased in Sahara the precipitation decreased in that area, but increased at the south. This rainfall shifting is mainly due to the change of the southwest Atlantic monsoon. We are not able to simulate that process in this study. Therefore, we can not find this feature in our experimnts. It might be one of the major deficiency for this 2–D model experiment.

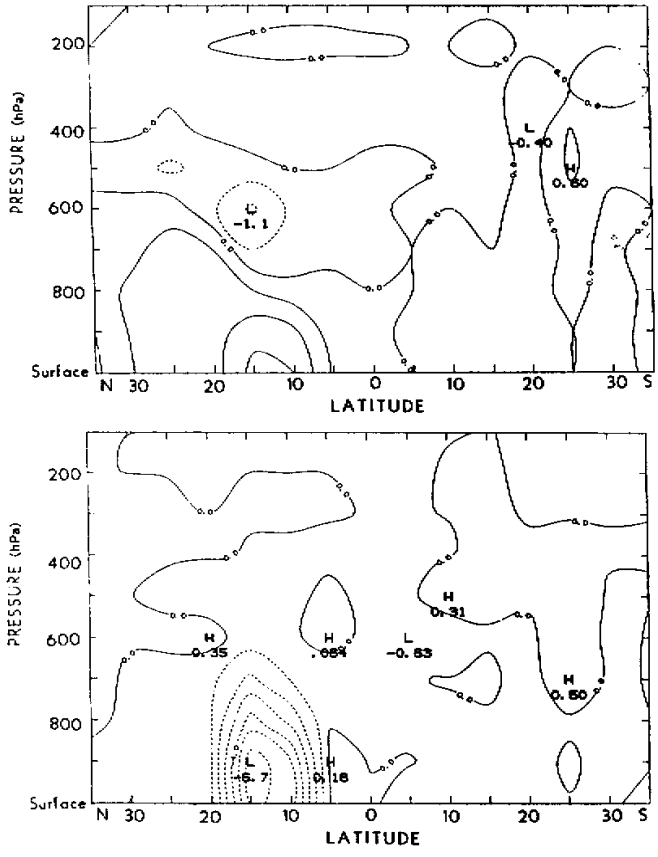

Fig.5. (a) Difference of temperature (K) between Case B and control run, the interval is 0.5 K, (b) Difference of water vapor specific humidity (g / kg) between Case B and control run. The interval is 0.5 g / kg.

The Fig.5 shows the difference of the temperature and humidity between anomaly run and control run for Case B. There are similar results for Case A with the opposite signs (not shown). After desert expanded the surface temperature at tested area increased 1.0–1.5 K. While the desert was removed, the surface temperature decreased about 0.5–1.0 K. However, in the middle troposphere the change had different signs. These are due to the loss or gain of net radiation in the top of the atmosphere. When the desert removed, the net radiation at the top of the atmosphere gained 8.1 w / m^2 in the tested area. After desertification the net radiation lost 3.2 w / m^2. The gain (loss) of the net radiation produced enhancement (decrease) of the temperature in the middle troposphere while the surface temperatures were directly affected by the surface energy balance. In fact, this is exactly what Charney predicted would happen after desertification (Charney et al., 1977). From Fig.5 b we can find the decreases of the water vapor in the atmosphere after desertification. Since water vapor concentrated in the lower troposphere, the significant differences were also confined in lower levels.

Another important feature is the change of the wind field. After desertification the sur-

face wind became strong. It increased 0.97 m / s. After desert removed, the surface wind speed decreased 0.32 m / s. The main features we discussed here are similar to the results with diurnal variations (Xue et al., 1990). However, without diurnal variation we may save a lot of computer time. It might be especially important while we want to make a very long period integration for climate study.

VI. CONCLUSION

This paper presented a two–dimensional model with the vegetation–soil layers in it. The biosphere model in this study is basically from BATS with some simplicity. We outlined the main structure and key parts in the vegetation model. The preliminary results from the coupled model have been discussed.

The very briefly discussion showed that the impact from surface to atmosphere is reasonable from this model and the impact of surface process on the atmosphere is significant. Although the 2–D model has its weakness, e.g., it omitted the zonal circulation and it might be crucial in some circumstances, it still provides a simple way to study physical feedback.

I thank Dr. Liou for his helpful comments on the paper.

REFERENCES

Charney, J. G (1975), Dynamics of deserts and drought in the Sahel, *Quart J. Roy. Meteor. Soc.*, **101**: 193–202.

Charney, J. G., W. K. Quirk, S.–H. Chow and J. Kornfield (1977), A comparative study of the effects of albedo change on drought in semi–arid regions, *J. Atmos. Sci.*, **34**: 1366–1385.

Deardorff, J. W. (1972), Theoretical expression for the countergradient vertical heat flux, *J. Geophys. Res.*, **77**: 5900–5904.

Deardorff, J. W. (1978), Efficient prediction of ground surface temperature and moisture, with inclusion of a layer of vegetation, *J. Geophys. Res.*, **83**: 1889–1908.

Dickinson, R. E. (1984), Modeling evapotranspiration for three–dimensional global climate models, In Chimate Processes and Climate Sensitivity, *Geophysical Monograph*, **29** (J. E. Hansen and T. Takahasi, Eds.), American Geophysical Union, Washington, D. C., 58–72.

Dickinson, R. E., and A. Henderson–Sellers (1988), Modelling tropical deforestation: A study of GCM land–surface parameterizations, *Quart J. Roy. Meteor. Soc.*, **114**: 439–462.

Dickinson, R. E., A. Henderson–Sellers, P. J. Kennedy and M. F. Wilson (1986), Biosphere–Amosphere Transfer Scheme (BATS) for the NCAR Community climate Model, NCAR / TN–275+STR.

Dickinson, R. E., J. Jager, W. M. Washington and Wolski (1981), Boundary Subroutine for the NCAR Global Climate Model, NCAR / TN–173+1A.

Haltiner, G. J., and R. T. Williams (1980), *Numerical Prediction and Dynamic Meteorology*, Wiley & Sons, New York, 471 pp.

Holloway, J. L., Jr., and S. Manabe (1971), Simulation of climate by a global general circulation model, *Mon. Wea. Rev.*, **99**: 335–370.

Liou, K. N. and S. C. S. Ou (1981), Parameterization of infrared radiative transfer in cloudy atmospheres, *J. Atmos. Sci.*, **38**: 2707–2716.

Liou, K. N. and S. C. S. Ou (1983), Theory of equilibrium temperatures in radiative–turbulent atmospheres, *J. Atmos. Sci.*, **40**: 214–219.

Matthews, E (1985), Atlas of archived vegetation, land–use and seasonal albedo data sets, *NASA Tech. Mem.*, 86199.

Oliger, J. E., R. E. Wellck, A. Kasahara and W. M. Washington (1970), Description of NCAR global circulation model, NCAR / TN–56+STR, 93 pp.

Oort, A. H. (1983), *Global atmospheric circulation statistics, 1958–1973.* NOAA Professional Paper No. 14, U. S. Government Printing Office, Washington, D. C., 180 pp. and 47 microfiches.

Sato, N., P. J. Sellers, D. A. Randall, E. K. Schneider, J. Shukla, J. L. Kinter, III, Y. –T. How and E. Albertazzi (1989), Effects of implementing the simple biosphere model in a general circulation model, *J. Atmos. Sci.*, **46**: 2757–2782.

Sellers, P. j., Y. Mintz, Y. C. Sud and A. Dalcher (1986), A simple biosphere model (SIB) for use within general circulation models, *J. Atmos. Sci.*, **43**: 505–531.

Shukla, J., C. Nobre and P. J. Sellers (1990), Amazonia deforestation and climate change, *Science*, **215**: 1498–1501.

Xue, Y. (1988), Investigation of the biogeophysical feedback on the African climate using a two–dimensional model, Ph.D. dissertation, University of Utah, 169 pp.

Xue, Y., K. N. Liou and A. Kasahara (1990), Investigation of the biogeophysical feedback on the african climate using a two–dimensional model, *J. Climate*, **3**: 337–352.

Xue, Y., P. J. Sellers, J. L. Kinter, III, J. Shukla (1990), A simplified biosphere model for global climate studies, *J. Climate, in press.*